TJER

A Quick and Comprehensive Method for Determining Static ATC with NRS and VFT

M. Eidiani
Energy Security and Sustainable Energy Institute, Mashhad, Iran

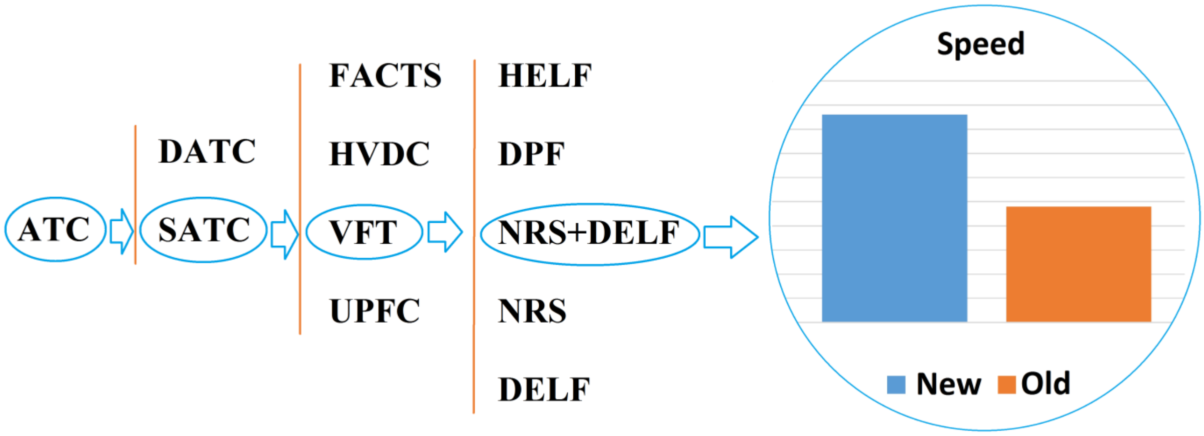

ABSTRACT: Electricity market players prioritize available transfer capability (ATC) as an attractive solution. Market participants can gain a financial advantage through accurate and fast ATC solutions. In order to provide a suitable and valuable solution, we use differential load flow equations. A dynamic system's entire time-domain trajectory can be solved by this method, along with a fictional time-domain differential equation. This article uses Newton-Raphson-Seydel instead of Newton-Raphson, which can also be used to determine voltage stability. A variable frequency transformer (VFT) was used in this study to increase and control transmission power. A 50% time saving on small systems was achieved with the proposed method, which was applied to seven different systems. In addition, it performed better on large systems by more than 90%. This proposal for static ATC presents promising results and can be applied to online applications.

الملخص: يُعْطِي المَعْنِيُّونَ فِي سُوقِ الكَهْرُباءِ أَوْلَوِيَّةً لِلقُدْرَةِ التَحْوِيلِيَّةِ المُتاحَةِ (ATC) بِاعْتِبارِها حَلّاً جَذّاباً. يُمْكِنُ لِلمُشارِكِينَ فِي السُوقِ الحُصُولُ عَلَى مِيزَةٍ مالِيَّةٍ مِن خِلالِ حُلُولِ ATC دَقِيقَةٍ وَسَرِيعَةٍ. لِتَقْدِيمِ حَلٍّ مُناسِبٍ وَقِيَمٍ، نَسْتَخْدِمُ مُعادَلاتِ تَدَفُّقِ الحَمْلِ التَفاضُلِيِّ. يُمْكِنُ حَلُّ مَسارِ الزَمَنِ الكامِلِ لِنِظامٍ دِينامِيكِيٍّ بِاسْتِخْدامِ هٰذِهِ الطَرِيقَةِ، إِلَى جانِبِ مُعادَلَةٍ تَفاضُلِيَّةٍ فِي المَجالِ الزَمَنِيِّ الوَهْمِيِّ. يَسْتَخْدِمُ هٰذا المَقالُ طَرِيقَةَ نْيُوتِن-رافسون-سيدُلُّ بَدَلاً مِن نْيُوتِن-رافسون، وَالَّتِي يُمْكِنُ أَيْضاً اِسْتِخْدامُها لِتَحْدِيدِ اِسْتِقْرارِ الجُهْدِ. تَمَّ اِسْتِخْدامُ مُحَوِّلِ التَرَدُّدِ المُتَغَيِّرِ (VFT) فِي هٰذِهِ الدِراسَةِ لِزِيادَةِ وَالتَحَكُّمِ فِي قُوَّةِ النَقْلِ. تَمَّ تَحْقِيقُ تَوْفِيرٍ زَمَنِيٍّ بِنِسْبَةِ 50% عَلَى الأَنْظِمَةِ الصَغِيرَةِ بِاسْتِخْدامِ الطَرِيقَةِ المُقْتَرَحَةِ، وَالَّتِي تَمَّ تَطْبِيقُها عَلَى سَبْعَةِ أَنْظِمَةٍ مُخْتَلِفَةٍ. بِالإِضافَةِ إِلَى ذٰلِكَ، أَدَّتْ بِشَكْلٍ أَفْضَلَ عَلَى الأَنْظِمَةِ الكَبِيرَةِ بِأَكْثَرَ مِنْ 90%. هٰذا الاِقْتِراحُ لِـ ATC الثابِتُ يُقَدِّمُ نَتائِجَ واعِدَةً وَيُمْكِنُ تَطْبِيقُهُ عَلَى التَطْبِيقاتِ المُباشِرَةِ.

Keywords: Available Transfer capability, Variable Frequency Transformer, Voltage Stability, Differential equation.

الكلمات المفتاحية: القدرة التحويلية المتاحة؛ محوّل التردد المتغير؛ استقرار الجهد؛ المعادلة التفاضلية.

Corresponding author's e-mail: eidiani@ijesse.net

DOI:10.53540/tjer.vol.20iss1pp45-51

NOMENCLATURE

A:	DEPF Jacobian matrix
B:	End variables in the DEPF LF
B:	DEPF load change in each direction
F_{new}:	New LF equations
g_{depf}:	DEPF general form of LF
J_{new}:	New Jacobian matrix
P_L:	Output power
P_d:	Mechanical power of the drive system
P_g:	Input power to the rotor
R_s, R_r: X_m, X_s:	VFT impedance
V_g, V_L: I_g, I_L:	Voltage and current of both sides of VFT
X_{old}:	Old network variables
X_{new}:	New general variables
X_{VFT}:	VFT variables
Y_{VFT}:	VFT admittance matrix
Z_{VFT}:	VFT impedance matrix
y_0:	NRS initial node injection
w:	DEPF decompose the voltage
λ,υ:	Eigenvalues and eigenvectors
θ_{rs}:	The angle of the rotor relative to the stator
θ_L, θ_g:	VFT voltage angle
P:	NRS search direction
A:	NRS scaled search parameter
Ψ:	DEPF loading parameter
X:	NRS general variables
Ξ:	NRS load flow
Θ:	NRS Hessian matrix

INTRODUCTION

Energy sources are maximized by interconnecting power grids with asynchronous and synchronous methods (Khan *et al.* 2021). Asynchronous and synchronous connections are made with HVAC and HVDC transmission lines, respectively. As the backbone of the future transmission network, HVDC lines are considered in ATC calculations. HVDC transmission lines allow large amounts of power to be transferred, but the design and analysis of HVDC systems are quite complex and expensive (Khan *et al.* 2021).

Power can be exchanged between two asynchronous or synchronous networks using a variable frequency transformer (VFT) (Khan *et al.* 2021). The first VFT was installed and tested by GE in Langlois in 2004. With the VFT, power between electrical networks can be controlled more easily than before (Merkhouf *et al.* 2006). Assumed in this paper is that one VFT in the network determines optimal power transmission.

It has long been an important issue in power system operation to calculate and send ATC every hour - both static ATC (SATC) (Liu et *al.* 2020, Eidiani et *al.* 2010) and dynamic ATC (DATC) (Eidiani 2021). DATC calculations are highly dependent on transient and voltage stability analysis (TSA-VSA) (Mohammed et *al.* 2019).

A general minimum residual method (GMRES) (Eidiani et *al.* 2010) can still be used to improve continuation power flow (CPF) (Zambroni et *al.* 2000) computations in SATC. The advantage of Newton-Raphson-Seydel (NRS) over NR is its faster and more accurate calculation of VSA and SATC (Eidiani et *al.* 2010).

ATC solution methods have been improved by incorporating artificial intelligence (AI) techniques into the optimal power flow calculation (OPF) (Lai et *al.* 1997). The ATC calculation was carried out using several AI methods, including cuckoo search, artificial neural networks, genetic and bee algorithms and particle swarm optimization (Lai et *al.* 1997).

Total transfer capability's (TTC) first contingency was limited by the high calculation time needed to compute unstable equilibrium points. ATC can be approximated with acceptable speed and accuracy using the Jacobian matrix determinant, transient stability and peak of potential energy method (Kim et *al.* 2009).

The DATC calculation with renewable sources on networks was presented using the support vector regression (SVR) method from 2012 to 2020 (Shaban 2018). A probabilistic power flow (PPF) approach for accessing SATC was proposed in (Karuppasamypandiyan et *al.* 2020). According to the results, this method provides a more accurate and effective evaluation of SATC.

An optimal power flow problem under transient stability constraints (TSC-OPF) can be used to estimate total transfer capability (Zhang et *al.* 2020). The state estimation program should also be used to calculate load flow (LF) parameters (Eidiani 2021).

There is no simplification or initial guessing required with the holomorphic embedding power flow (HEPF) algorithm (Eidiani 2021), although it has a long computation time. Using the differential LF approach, transient stability simulations can be solved effectively (Eidiani 2021). A numerical algorithm that does not require iteration is developed by the researchers in (Eidiani 2021) in order to solve nonlinear AC load flows. An embedding of differential equation power flow (DEPF) into the proposed method (SATC-DE) was used in the current work. Additionally, this study used DEPF (Eidiani 2021)'s initial model and improved the method of calculating Static ATC (SATC). With the developed model, large and practical systems can be analyzed with less computational overhead and consistent performance.

We describe here the key characteristics of the new SATC evaluation method with VFT. We developed a differential equation-based SATC calculation in the presence of VFT in this study. The new algorithm is based on the initial work on the differential equation LF algorithm that was published in (Eidiani 2021), which showed efficiency in terms of dynamic LF. In section 2, DEPF with NRS and VFT model is defined, and in section 3, the proposed approach for SATC assessment with VFT is discussed. The fourth section presents the results and discussions.

Lastly, the proposed method is tested on several bi- and multilateral contract systems.

DEPF WITH NRS AND VFT MODEL

An illustrated network connection for VFT can be seen in Figure 1, and a simplified circuit diagram for VFT can be seen in Figure 2.

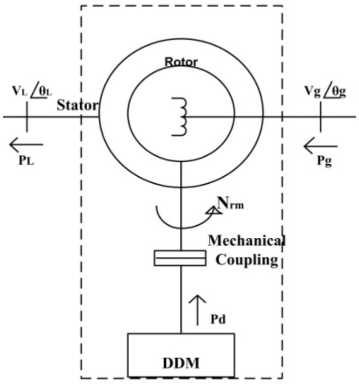

Figure 1. An illustrated network connection for VFT (Khan *et al.* 2021)

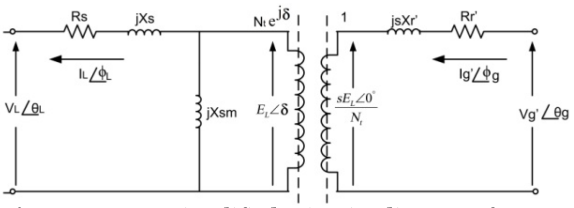

Figure 2. A simplified circuit diagram for VFT (Merkhouf *et al.* 2006)

The relationship between P_g, P_d, and P_L is shown in Figure 1. P_L is the output power, P_d is the mechanical power of the drive system, and P_g represents the input power to the rotor.

$$P_g+P_d=P_L \tag{1}$$

The following are bipolar equations that can be used to calculate VFT's voltage and current equations (Figure 2).

$$\begin{bmatrix} V_g \\ V_L \end{bmatrix} = \left[Z_{VFT}\right]\begin{bmatrix} I_g \\ I_L \end{bmatrix} \Rightarrow \quad \begin{bmatrix} I_g \\ I_L \end{bmatrix} = \left[Y_{VFT}\right]\begin{bmatrix} V_g \\ V_L \end{bmatrix} \tag{2}$$

Equation (2) can be applied to the LF equation, and the VFT angle (δ) can be varied to adjust the transfer power between the rotor and stator. Increased ATC can be achieved by controlling power at the VFT, which then controls power at the transmission line.

It should be noted that in a VFT, where torque is applied to the rotor, the induced Emf in the coil of the rotor remains constant, but its phase angle changes by θ_{rs}. The following real equations are obtained by simplifying the LF equations in Figure 2.

$$\begin{aligned}
V_L \sin\theta_L &= I_g X_m \cos(\phi_g+\theta_{rs}) - I_L X_s \cos\phi_L \\
&\quad - I_L X_m \cos\phi_L - I_L R_s \sin\phi_L \\
V_L \cos\theta_L &= I_g X_m \sin(\phi_g+\theta_{rs}) + I_L X_s \sin\phi_L \\
&\quad - I_L X_m \sin\phi_L - I_L R_s \cos\phi_L \\
V_g \sin(\theta_{rs}+\theta_g) &= (X_m+X_r) s I_g \cos(\theta_{rs}+\phi_g) \\
&\quad - I_L X_m s \cos\phi_L + I_g R_r \sin(\theta_{rs}+\phi_g) \\
V_g \cos(\theta_{rs}+\theta_g) &= -(X_m+X_r) s I_g \sin(\theta_{rs}+\phi_g) \\
&\quad + I_L X_m s \sin\phi_L + I_g R_r \cos(\theta_{rs}+\phi_g)
\end{aligned} \tag{3}$$

The main LF equations can be easily modified by deriving LF flow equations (3). We can replace old network variables ($X_{old}=[\delta, V]^t$) with new general variables ($X = X_{new} = [X_{old}, X_{VFT}]^t$) by defining VFT variables as ($X_{VFT} = [\theta_L, \theta_g, \theta_{rs}, V_L, V_g]^t$). It is now possible to calculate the new LF equations and the new Jacobian matrix of the network.

$$F_{new}(X_{new}) = 0 \Rightarrow \Delta F_{new} = J_{new}\,\Delta X_{new}$$
(4)

Or:

$$\Delta F_{new} = J_{new}\,\Delta X_{new}$$
$$\Rightarrow \begin{bmatrix} \Delta P \\ \Delta Q \\ \Delta T \end{bmatrix} = \begin{bmatrix} J_{P\theta} & J_{PV} & J_{PX_{VFT}} \\ J_{Q\theta} & J_{QV} & J_{QX_{VFT}} \\ J_{T\theta} & J_{TV} & J_{TX_{VFT}} \end{bmatrix} \begin{bmatrix} \Delta\theta \\ \Delta V \\ \Delta X_{VFT} \end{bmatrix}$$
(5)

NRS load flow can now be used to solve equation (6) (Eidiani et *al.* 2010) $\chi = [X \;\; \nu \;\; \alpha]^t$.

$$\Xi(\chi) = \begin{bmatrix} J_{new}\nu - \lambda\nu \\ 1 - \|\nu\| \\ y_0 + \rho\alpha + F_{new}(X) \end{bmatrix} = 0 \Rightarrow$$

$$\Rightarrow \frac{\partial \Xi}{\partial \chi} = \Xi_\chi(\chi) = \begin{bmatrix} \Theta & J_{new} - \lambda I & 0 \\ 0 & \frac{\nu'}{\|\nu\|} & 0 \\ \frac{\partial F_{new}}{\partial X} & 0 & -\rho \end{bmatrix} \tag{6}$$

That:

$$\Theta = \frac{\partial^2 F_{new}}{\partial X_{new}^2} \times \begin{bmatrix} \nu_1 & & 0 \\ & \ddots & \\ 0 & & \nu_n \end{bmatrix} = \begin{bmatrix} \frac{\partial}{\partial X_{1new}} J_{new}.\nu \\ \vdots \\ \frac{\partial}{\partial X_{n\,new}} J_{new}.\nu \end{bmatrix} \tag{7}$$

And:

$$inv\left(\Xi_\chi(\chi)\right)=\begin{bmatrix}\Theta & \Xi_{\chi12}\\ \Xi_{\chi21} & \Xi_{\chi22}\end{bmatrix}^{-1}$$
$$=\begin{bmatrix}\Theta^{-1}(I+\Xi_{\chi12}\Xi_*\Xi_{\chi21}\Theta^{-1}) & -\Theta^{-1}\Xi_{\chi12}\Xi_*\\ -\Xi_*\Xi_{\chi21}\Theta^{-1} & \Xi_*\end{bmatrix} \quad (8)$$
$$\Xi_*=(\Xi_{\chi22}-\Xi_{\chi21}\Theta^{-1}\Xi_{\chi12})^{-1}$$

The NRS equation can now be combined with the DEPF equation. The proposed method solves a linear equation only once per time step, whereas the CPF method solves it in every correction-prediction step. We now briefly review the DEPF approach (Eidiani 2021). DEPF calculations are based on the concept of converting continuous-time parameters into discrete variables like (w(t) ↔ W(k)). The normal LF is depicted in (9), where (b) is the load change in each direction and ψ is the loading parameter.

$$I=YV \Rightarrow S=VI^*=V(YV)^* \Rightarrow$$
$$S+\psi b=VY^*V^* \quad (9)$$

In order to decompose the voltage, we need to do the following:

$$w=[real(V),imaginary(V)] \quad (10)$$

It is now possible to write (10) as (11) in the general form.

$$g_{depf}(\psi,w)=0 \quad (11)$$

DEPF defines a reversible relationship for changing variables as (12).

$$w(t)=\sum_{k=0}^{K}(t^kW(k))\Leftrightarrow W(k)=\frac{1}{k!}\left[\frac{d^kw(t)}{dt^k}\right]_{t=0} \quad (12)$$

First, the DEPF method expands the algebraic equation (11) by adding a state variable (x) to a set of DAEs. We obtain the following linear equation by linearizing all the equations using (12). As a result, we can obtain the Jacobian matrix of the method as follows (Eidiani 2021):

$$\begin{bmatrix}W(k)\\ \Psi(k)\end{bmatrix}=\begin{bmatrix}A_{12} & A_{12}\\ A_{21} & A_{22}\end{bmatrix}^{-1}\begin{bmatrix}B_1\\ B_2\end{bmatrix} \quad (13)$$

The nonlinear LF equation (14) is solved using ($A_1A_2A_3A_4$) matrices in a differential transformation (Eidiani 2021). We have:

$$\begin{bmatrix}W(k)\\ \Psi(k)\end{bmatrix}=$$
$$=\begin{bmatrix}A_{11}^{-1}(I+A_{12}A_*A_{21}A_{11}^{-1}) & -A_{11}^{-1}A_{12}A_*\\ -A_*A_{21}A_{11}^{-1} & A_*\end{bmatrix}^{-1}\begin{bmatrix}B_1\\ B_2\end{bmatrix} \quad (14)$$
$$A_*=(A_{22}-A_{21}A_{11}^{-1}A_{12})^{-1}$$

DEPF model's key characteristics helped us find a simple and user-friendly SATC solution in an accurate and fact manner.

THE PROPOSED METHOD OF SATC

LFs are calculated using the DEPF approach at the contract update with a decrease or increase in loading parameters. SATCs have been determined for normal and contingency cases. An algorithm for assessing SATC using DEPF, NRS, and VFT can be seen in the following.

1- All network information, controllers, and sales contracts should be entered.
2- For each bi/multilateral contract (i) between seller and buyer, change the vector of load direction in (9) accordingly.
3- Utilize the DEPF method developed in the previous section of this contract to find the maximum load parameter.
4- In this contract, calculate the ATC for normal and contingencies.
5- Using the previous steps, determine the maximum allowable transmission power between buyer and seller.
6- At each contract, evaluate SATC.
7- If the type of contract is changed, the algorithm goes back to step 1 until the final contract.

It is similar to the previous section in the SATC calculation after the generator is lost or disconnected, except the bus type changes to PQ. A parallel line with negative impedance can also simulate a line disconnected. Lines and transformers have a maximum thermal load limit of 100%, active power of 0 to 90%, a reactive power of 50% to -50%, and a maximum voltage difference of 5%. This method shows high speed and accuracy in several networks based on the above conditions.

RESULTS AND DISCUSSIONS

DIgSILENT PowerFactory and MATLAB were used to simulate the proposed SATC model. We studied developed mode performance on a computer with Core i7 (Intel), 2 cores, 2.3GHz, 8GB RAM. We tested the proposed SATC on a number of systems, including 40 (Link 1), 120 (Link 1), 150 (Eidiani 2021), 300 (Link 1), 4440 and 1150 (Liu et *al.* 2020) and 6070 (Link 2). Several approaches are compared with the simulation results of the new method, including HEPF (Eidiani 2021), NRS (Eidiani et *al.* 2010), SATC (Eidiani 2021), CPF-GMRES (Eidiani et *al.* 2010) and CPF (Zambroni et *al.* 2000).

SATC solutions calculated using six methods, seven systems and four multilateral and 21 bilateral transactions are shown in Table 1. A comparison was made between the proposed method's Root Mean Square Error (RMSE) and Calculate Relative Speed (CRS) (Table 2). There is no direct correlation between the number of buses and the CRS. In terms of execution time, the proposed method outperforms other approaches. It was found that the new method consumed nearly half the processing time compared to the other methods on average. As shown in Table 2, even if there is VFT, the proposed method is faster than the usual methods.

Figure 6 illustrates the root mean square errors between the proposed method and the other approaches, both with and without the VFT. The accuracy of the SATC solution found by all approaches varies from 0.08% to 2%, compared with the accuracy of ATC calculated based on CPF. In comparison to conventional methods, the proposed method takes almost 40% to 60% less time to calculate SATC, and 8% less time than HEPF. In comparison with the contender methods, 65 to 90% of the time can be saved, as well as 15% more than with HEPF.

The outcome of the study indicates that the proposed approach facilitates the computation of SATC calculations that are nearly 25% to 90% computationally efficient, proving that the developed model is both practical and suitable for online use.

Based on the simulation results, the most precise method is the conventional CPF method used as a benchmark. CPF, on the other hand, is the closest approach to the new method. In addition, the developed approach was shown to be readily applicable for distribution systems as well, thus extending its robustness beyond transmission networks.

Table 2. Comparing the CRS of the proposed method with other methods with and without VFT, Methods (M.) and systems (S.) are similar to Table 1

S.	M1		M2		M3		M4		M5	
	W/o	W/.	W/o	W/.	W/o	W/.	W/o	W/.	W/o	W/.
1	57	70	51	67	39	59	35	56	9	35
2	94	96	86	91	67	79	61	75	14	42
3	90	94	83	89	64	77	58	72	18	41
4	82	88	80	87	58	72	52	68	20	45
5	68	77	70	80	48	63	48	63	21	43
6	56	70	59	72	42	60	38	57	32	53
7	55	69	57	71	50	65	48	64	46	63

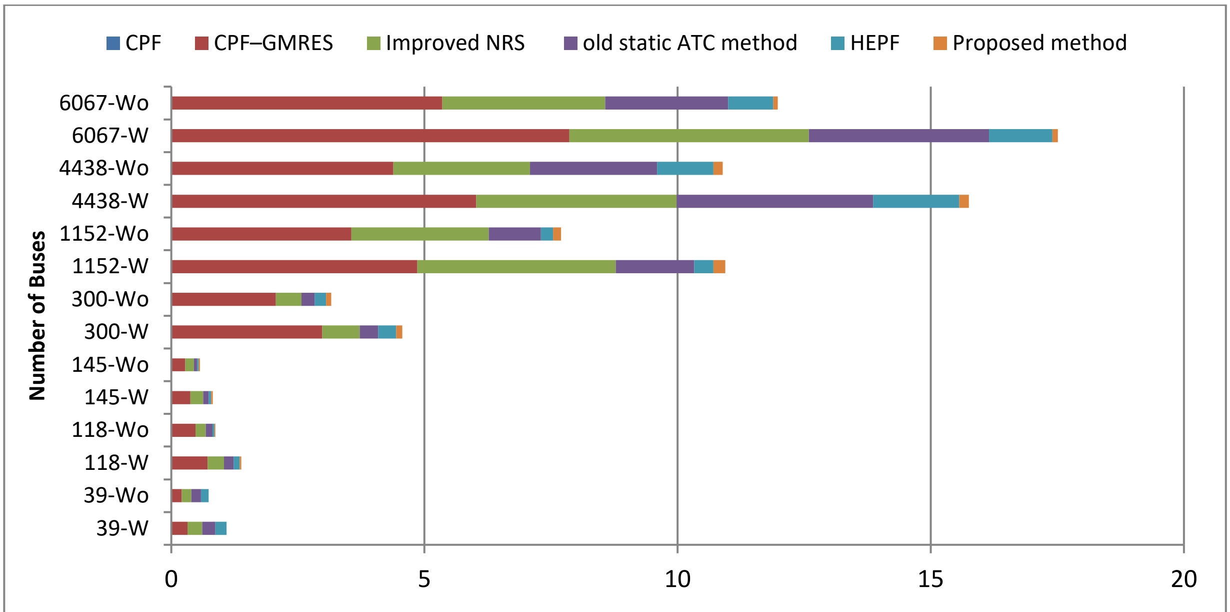

Figure 3- Comparing the proposed method with other methods with and without VFT

Table 1. SATC (p.u.) and Error (Er), with (W/.) and without (W/o) VFT Methods (M.): 1-CPF (Zambroni et *al.* 2000), 2-CPF-GMRES (Eidiani et *al.* 2010), 3- NRS (3) (Eidiani et *al.* 2010), 4- SATC (4) (Eidiani 2021), 5- HEPF (5) (Eidiani 2021) and 6- The proposed method. Systems (S.): 1-40 (Link 1), 2-120 (Link 1), 3-150 (Eidiani 2021), 4-300 (Link 1), 5-1150 and 6-4440 (Eidiani 2021) and 7-6070 (Link 2).

S.	M.	RMSE W/o-W/.	SATC		Error		SATC		Error		SATC		Error		SATC		Error	
			W/o	W/.	W/o	W/.	W/o	W/.	W/o	W/.	W/o	W/.	W/o	W/.	W/o	W/.	W/o	W/.
Contract			Sell (30) and Buy (7)				Sell (30) and Buy (4)				Sell (30,31) and Buy (18,20)				Sell (30) and Buy (3)			
1	1	0.0	643	780	0.0	0.0	83	109	0.0	0.0	425	593	0.0	0.0	126	174	0.0	.0
	2	0.21-0.32	645	784	0.31	.49	84	109	0.12	.17	426	595	0.24	.37	126	174	0.08	.12
	3	0.19-0.29	642	782	0.16	.25	83	109	0.24	.38	424	595	0.24	.35	126	174	0.08	.11
	4	0.19-0.26	642	778	0.16	.21	83	109	0.24	.33	424	591	0.24	.31	126	174	0.08	.12
	5	0.15-0.22	644	778	0.16	.22	83	109	0.12	.18	424	591	0.24	.34	126	174	0.0	0.0
	6	0.0	643	780	0.0	0.0	83	109	0.0	0.0	425	593	0.0	0.0	126	174	0.0	0.0
Contract			Sell (89) and Buy (23)				Sell (89) and Buy (83)				Sell (89,87) and Buy (23,83)				Sell (89) and Buy (75)			
2	1	0.0	278	358	0.0	0.0	285	373	0.0	0.0	286	369	0.0	0.0	310	390	0.0	0.0
	2	0.48-0.72	279	356	0.47	.68	284	372	0.14	.19	284	373	0.67	1.05	312	393	0.48	.70
	3	0.20-0.32	278	357	0.18	.25	284	379	0.32	.49	285	370	0.18	.28	310	391	0.03	.20
	4	0.13-0.19	277	357	0.18	.24	285	374	0.04	.13	286	368	0.11	.15	310	389	0.16	.21
	5	0.04-0.12	277	358	0.04	.05	285	374	0.04	.18	286	369	0.04	.06	310	391	0.03	.13
	6	0.02-0.03	278	358	0.0	.01	285	373	0.04	.06	286	369	0.0	0.02	310	390	0.0	0.0
Contract			Sell (33) and Buy (149)				Sell (32) and Buy (108)				Sell (34) and Buy (20,63)				Sell (31) and Buy (91)			
3	1	0.0	426	575	0.0	0.0	664	810	0.0	0.0	299	366	0.0	0.0	755	961	0.0	0.0
	2	2.06-2.98	418	592	1.91	2.90	677	788	1.92	2.75	308	351	2.92	4.14	747	946	1.07	1.53
	3	0.51-0.74	424	579	0.47	0.70	662	807	0.30	.39	301	370	0.66	1.02	759	954	0.53	.71
	4	0.26-0.37	425	577	0.24	.38	663	808	0.15	.20	298	364	0.34	.48	753	958	0.27	.36
	5	0.23-0.35	425	577	0.24	.36	663	808	0.15	.21	298	368	0.34	.53	754	960	0.13	.17
	6	0.10-0.12	426	575	0.0	.07	665	811	0.15	.17	299	366	0.0	0.03	756	960	0.13	.14
Contract			Sell (43) and Buy (142)				Sell (42) and Buy (139)				Sell (44) and Buy (141,143)				Sell (41) and Buy (132)			
4	1	0.0	449	600	0.0	0.0	388	506	0.0	0.0	502	697	0.0	0.0	324	443	0.0	0.0
	2	.28-0.38	447	597	0.31	.42	387	504	0.26	.34	500	701	0.34	.52	325	442	0.15	.21
	3	.17-0.25	448	602	0.18	.29	387	504	0.23	.31	503	695	0.18	.26	324	443	0.03	.05
	4	.06-0.11	449	599	0.02	.11	388	507	0.08	.12	502	697	0.04	.06	325	442	0.09	.12
	5	.03-0.05	449	600	0.0	.06	388	506	0.05	.07	502	697	0.02	.04	324	443	0.03	.04
	6	.02-0.03	449	600	0.0	.04	388	506	0.03	.04	502	697	0.0	0.0	324	443	0.03	.04
Contract			Sell (t400) and Buy (d132)				Sell (sh400) and Buy (b132)				Sell (t400,f400), Buy (s132)				Sell (f400) and Buy (f132)			
5	1	0.0	485	625	0.0	0.0	945	1168	0.0	0.0	557	724	0.0	0.0	877	1178	0.0	0.0
	2	3.56-4.86	466	592	4.08	5.39	972	1124	2.78	3.78	585	677	4.79	6.55	861	1212	1.86	2.89
	3	2.71-3.92	470	654	3.19	4.69	928	1140	1.83	2.44	537	764	3.72	5.48	890	1156	1.42	1.87
	4	1.03-1.55	480	616	1.04	1.44	942	1163	0.32	.43	548	743	1.64	2.59	872	1168	0.57	.81
	5	0.24-0.38	486	627	0.21	.32	947	1172	0.21	.33	555	728	0.36	.58	876	1176	0.11	.15
	6	0.16-0.23	484	624	0.21	.30	944	1169	0.11	.15	556	726	0.18	.28	876	1176	0.11	.14
Contract			Sell (134) and Buy (4257)				Sell (78) and Buy (3765)				Sell (195,186) and Buy (25,12)				Sell (25) and Buy (2221)			
6	1	0.0	478	676	0.0	0.0	363	499	0.0	0.0	578	731	0.0	0.0	591	723	0.0	0.0
	2	4.39-6.02	489	655	2.25	3.07	380	469	4.48	6.06	570	717	1.40	1.95	552	653	7.07	9.75
	3	2.70-3.96	471	662	1.49	2.15	357	512	1.68	2.63	557	692	3.77	5.38	573	757	3.14	4.73
	4	2.51-3.88	473	666	1.06	1.53	350	528	3.71	5.86	565	755	2.30	3.34	578	749	2.25	3.52
	5	1.11-1.70	482	667	0.83	1.09	356	514	1.97	3.06	576	735	0.35	.55	588	729	0.51	0.80
	6	0.18-0.19	478	675	0.0	0.22	362	497	0.28	.20	577	730	0.17	.15	590	721	0.17	.20
Contract			Sell (3) and Buy (162)				Sell (2) and Buy (632)				Sell (3,4) and Buy (570,942)				Sell (1) and Buy (943)			
7	1	0.0	984	1281	0.0	0.0	746	1012	0.0	0.0	879	1259	0.0	0.0	935	1244	0.0	0.0
	2	5.35-7.86	953	1222	3.23	4.65	710	939	5.11	7.24	863	1226	1.87	2.64	861	1405	8.63	12.9
	3	3.22-4.73	965	1321	1.98	3.11	730	980	2.22	3.19	845	1192	3.98	5.36	899	1324	4.11	6.40
	4	2.43-3.56	973	1305	1.21	1.89	723	969	3.23	4.21	858	1309	2.49	3.96	914	1290	2.34	3.70
	5	0.89-1.25	978	1294	0.67	1.01	736	993	1.43	1.89	875	1269	0.49	0.76	927	1257	0.68	1.06
	6	0.09-0.11	984	1280	0.04	.06	745	1011	0.09	.12	878	1260	0.09	.14	934	1243	0.11	.11

CONCLUSION

A new algorithm based on differential power flow equations and Newton-Raphson-Seydel was developed to calculate static available transmission capacity. In this paper, a power controller called a Variable Frequency Transformer is used to increase power. This controller complicates calculations. Several test systems were examined, including standard IEEE systems as well as large-scale and practical utility systems, to demonstrate the method's ability. The new method increases calculation speed and reduces calculation error compared to existing methods with VFT. Accordingly, the proposed SATC method provides accurate results while taking less CPU time to complete than other methods. As a result, the proposed method has the potential to be applied online in large transmission and distribution networks with VFT.

CONFLICT OF INTEREST

The authors declare that there are no conflicts of interest regarding this article.

FUNDING

The research underpinning this publication was undertaken independently and was not contingent upon any external financial endorsements or grants.

REFERENCES

DIgSILENT GmbH. (n.d.). Power system software & engineering. Retrieved from https://www.digsilent.de

Dynamic IEEE Test Systems. (2020). Retrieved from https://www2.kios.ucy.ac.cy/testsystems/

Eidiani, M. (2021). A reliable and efficient holomorphic approach to evaluate dynamic available transfer capability. International Transactions on Electrical Energy Systems. 31(11), 1-14.

Eidiani, M., Zeynal, H., Zadeh, A.K., Nor, K.M. (2010, Nov. 29 – Dec. 1), Exact and Efficient Approach in Static Assessment of Available Transfer Capability (ATC). PECon2010, IEEE International Conference on Power and Energy, Kuala Lumpur, Malaysia, 189- 194.

Karuppasamypandiyan, M., Aruna Jeyanthy P., Devaraj, D., Agnes Idhaya Selvi, V., (2020), Day ahead dynamic available transfer capability evaluation incorporating probabilistic transmission capacity margins in presence of wind generators. International Transactions on Electrical Energy Systems. 1-21.

Khan, M.M., Jamel, I., Rahman, H. (2021), Research on Variable Frequency Transformer: A Smart Power Transmission Technology. IEEE Access. 9, 105588-105605.

Kim, K.H., Kim, S.N., Rhee, S.B., Lee, S.K., and Song, K.B., (2009, Oct. 26-30), Assessment of total transfer capability subject to transient stability energy margin. Transmission & Distribution Conference & Exposition: Asia and Pacific, Seoul, Korea (South), pp. 1-4,

Lai, L.L., Ma, J.T., Yokoyama, R., Zhao, M. (1997), Improved genetic algorithms for optimal power flow under both normal and contingent operation states. International Journal of Electrical Power & Energy Systems. 19(5), 287-292.

Liu, Y., Sun, K., Dong, J. (2020). A dynamized power flow method based on differential transformation. IEEE Access. 8, 182441–182450.

Merkhouf, A., Upadhyay, S., Doyon, P. (2006, June 18-22), Variable Frequency Transformer – An Overview. IEEE Power Engineering Society General Meeting. Montreal, Que. 1-4.

Mohammed, O.O., Mustafa, M.W., Mohammed, D.S.S., Otuoze, A.O. (2019), Available transfer capability calculation methods: A comprehensive review. International Transactions on Electrical Energy Systems. 29(6):1-24.

Shaaban, M., (2018), Behavior of Power System Equilibrium Points in Dynamic Available Transfer Capability Calculation. Journal of Applied Science & Process Engineering, 5(1): 242-248

Zambroni, A.C., and Souza, D., (2000), Discussion on some voltage collapse indices. Electric Power System Research, No. 53, 2000

Zhang, Y., Liu, W., Huan, Y., Zhou, Q., Wang, N. (2020), Online Dynamic Total Transfer Capability Estimation Using Co-training-Style Semi-Supervised Regression. IEEE Access. 8, 94054 - 94064.